Microstructural Characterization of Firn

I. BAKER[1], R. OBBARD[1], D. ILIESCU[1], AND D. MEESE[1,2]

ABSTRACT

In this paper, we use a scanning electron microscope (SEM) coupled with x-ray spectroscopy and electron back-scattered diffraction patterns to examine firn in cores retrieved by the United States International Trans-Antarctic Scientific Expedition. From grain boundary grooves we were able to see where the previously-existing snow crystals were joined, and can determine grain sizes. From the SEM images, the porosity and the surface area per unit volume of the pores were measured. Finally, we have shown that we can determine the microchemistry of impurities in firn and demonstrated that we can determine the orientations of the firn crystals.

Keywords: Firn, snow, porosity, surface area, scanning electron microscopy, x-ray microanalysis

INTRODUCTION

In a number of recent papers, we have used a scanning electron microscope coupled with energy-dispersive x-ray microanalysis (EDS) to determine the microstructural location of impurities in ice cores (Cullen and Baker 2000; 2001; 2002a; 2002b; Cullen et al. 2002; Iliescu et al. 2002; Baker et al. 2003; Baker and Cullen 2003a; 2003b; Obbard et al. 2003a; 2003b; Iliescu and Baker 2004; Baker et al. 2006). A key feature of this work is that the ice specimens were uncoated, and examined at -80 ± 10 °C so that slight sublimation from the ice prevented charge build-up. This is a technique that we have also used to examine snow (Iliescu and Baker 2002) and that Barnes and co-workers used to examine both ice cores and snow from Antarctica (Barnes et al. 2002a; 2002b; 2003). This approach has an advantage over the use of aluminum or gold coating on ice to prevent charging in the SEM (Mulvaney, Wolff and Oates 1988; Wolff, Mulvaney and Oates 1988; Barnes et al. 2002b) since the metal coatings can obscure weaker X-ray fluorescence signals from the sample.

In other work, we have demonstrated that Raman spectroscopy coupled with a confocal scanning optical microscope can be used to analyze impurities in grain boundaries and triple junctions that cannot be detected by EDS (Iliescu et al. 2004). MicroRaman spectroscopy was first used to look at impurities in a triple junction in ice by Fukazawa and co-workers (1998).

More recently, we have demonstrated that we can obtain the complete orientations of crystals in polycrystalline ice (not simply the *c*-axis direction) with high angular (0.1^{o}) and spatial resolution (50 nm) by using electron back-scattered patterns (EBSPs) obtained in a SEM (Iliescu et al. 2004; 2005; Obbard et al. 2006).

In this paper, we show, for the first time, that we can obtain SEM images, EDS and EBSPs from uncoated firn using the same approach. Ultimately, such information can provide an efficient and accurate method of measuring porosity, internal surface area and grain size and will allow us an

[1] Thayer School Of Engineering, Dartmouth College, Hanover, NH 03755, Email: Ian Baker (Ian.Baker@Dartmouth.Edu)
[2] Climate Change Institute, University Of Maine, Orono, ME 04469

understanding of how impurities are redistributed and how fabric forms in the shallow layers of ice sheets.

EXPERIMENTAL

We examined six firn specimens from depths of 9.71 m, 19.545 m and 34.465 m from core 02-SP, and depths of 13.019 m, 23.028 m and 38.533 m, from core 02-5 obtained on the United States International Trans-Antarctic Scientific Expedition (ITASE). Core 02-SP is at the South Pole while core 02-5 is the next core along the route, see the route map at http://www2.umaine.edu/USITASE/html/map.html for details.

For examination in the SEM, ~25-mm- × 25-mm- × 10-mm-thick specimens were cut perpendicular to the core axis, shaved flat with a razor blade under a HEPA-filtered, laminar-flow hood at -10°C and frozen onto a brass plate. Specimens were then either sealed in a small container for later examination or mounted onto a cold stage for immediate observation. For imaging and microanalysis, the uncoated specimens were examined at -80°C ± 10°C using a JEOL 5310 low-vacuum SEM operated at 10 kV equipped with a Princeton Gamma-Tech IMIX EDS system utilizing a lithium-drifted silicon thin-window detector. For orientation determination, specimens were frozen to a purpose-built pre-tilted brass sled that was then mounted on a cold stage in a field emission gun FEI XL-30 environmental SEM. The SEM was operated at 15 kV with a beam current of 0.15 nA, and the ice was again examined at temperatures between -80°C ± 10°C at a pressure of approximately 5×10^{-4} Pa. Secondary electron imaging was used on both SEMs. EBSPs were captured using the techniques described by Iliescu and others (Iliescu et al. 2004; 2005) and indexed using HKL Technologies' CHANNEL 5™ software.

RESULTS AND DISCUSSION

Figure 1 shows low-magnification secondary electron images of firn from three different depths. The images were obtained as soon as possible after the specimens were inserted into the SEM to reduce the degree of sublimation, which can affect the appearance of the specimens. Several features are worth noting. First, shaving the ice produced some debris, which fell into the pores in the ice. This was much more noticeable in the higher porosity shallow ice, presumably because the grains were less strongly bonded together and the pore volume is larger. Examples of such debris are labeled "D" in Figure 1(a).

Second, grain boundaries grooves were observed in some images. These indicate where the snow crystals are joined together, see Figure 1 (a). By allowing the specimens to sublimate in the SEM it is possible to see grain boundary grooves between all the individual ice crystals and, hence, it should be possible to determine how the grain size changes as a function of depth in the firn. However, one needs to be aware that longer sublimation times, due to loss of mass, drastically affect the appearance of the microstructure and hence a delicate compromise needs to be achieved between the need to depict the microstructure in an accurate unadulterated manner and the desired to better visualize the details within the grain boundary region.

Third, it is straightforward to determine the % areal porosity from these images by dividing the area occupied by the shaved flat regions by the area of the image. The pore area and length of boundary area were measured on the SEM images using Image SXM (Barrett 2005), a derivative of NIH Image (Rasband 1997). The boundaries of pore areas were traced with the drawing tool, and the perimeter and enclosed area measured with the pixel-counting measurement utility, see Figure 2. As is quite common in the SEM, the edges of the flat surface tended to charge. This analysis was performed from multiple images at each depth (except for the 9.71 m specimen, where only one image was available). The porosity values obtained at each depth are shown in Table 1. As might be expected, (except for the 9.71 m specimen), the porosity at a particular site decreases with increasing depth.

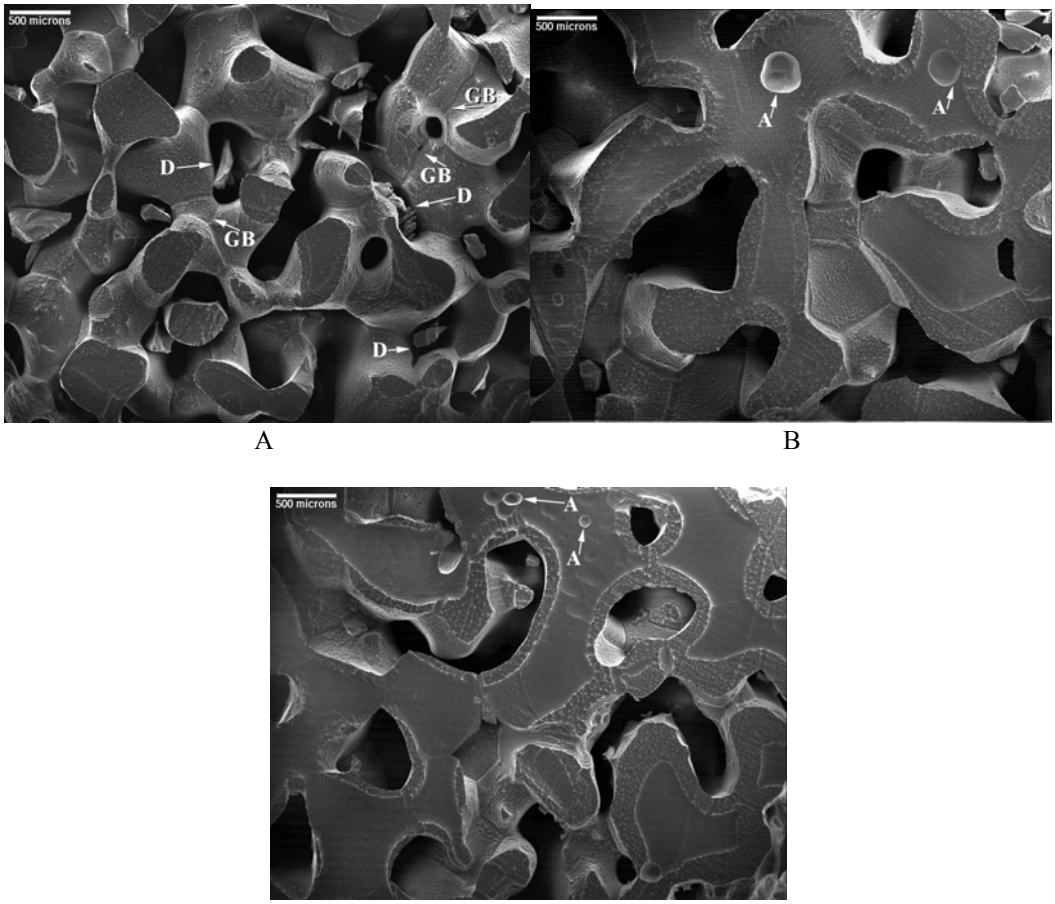

Figure 1. Low-magnification secondary electron images of firn samples from depths of (a) 9.71 m, (b) 23.028 m, and (c) 34.465 m. The features labeled "D" in (a) are debris produced by shaving. Some grain boundaries where the original snow crystals joined together, as indicated by grooves, are labeled "GB". Some air bubbles are indicated by "A".

Table 1. Porosity, measured length of internal surface around the pores in 16 mm2 areas, length of (internal surface) line per unit area, LA, and internal pore surface area per unit volume, SV, for various depths at two sites from the US ITASE measured from SEM images.

Site	Depth (m)	% Porosity	Measured length of surface (mm)	L_A (mm^{-1})	S_V (mm^{-1})
02-SP	9.71	80	33.2	2.08	2.65
02-5	13.019	85	28.7	1.79	2.28
02-SP	19.545	87	44.5	2.78	3.54
02-5	23.028	58	30.4	1.98	2.52
02-SP	34.465	36	40.7	2.54	3.23
02-5	38.533	38	40.6	2.54	3.23

Fourth, by measuring the length of the surface around the pores per unit area it is possible to obtain the internal surface area per unit volume, see Figure 2. Microstructural examinations are normally performed on firn by infiltrating the firn with a liquid, e.g. dimethyl Phthalate (Albert and Shultz 2002; Rick and Albert 2004), allowing it to set, and then sublimating the firn. The problems with this method are that the viscous liquid cannot easily penetrate small pores, which increase in frequency with depth; and, of course, the liquid cannot infiltrate closed off pores, which also increase in frequency with depth. The lengths of projected surface around the pores measured from images of area 16 mm^2 are shown along with the length of (internal surface) line per unit area, $\mathbf{L_A}$, in Table 1. The internal surface area per unit volume, $\mathbf{S_V}$, was calculated from $\mathbf{L_A}$ using: $\mathbf{S_V} = (4/\pi)\,\mathbf{L_A}$ (Underwood 1970). In contrast to the volume porosity, the internal surface area per unit volume of the pores was generally found to increase with increasing depth. This is an unexpected result. It may indicate that the pores are more convoluted at greater depth even though their percentage of the volume is less. A more detailed SEM analysis would involve taking both horizontal and vertical sections. This becomes more important with increasing depth where the pore and grain structures become more inhomogeneous due to the flattening of the microstructure from the increasing overburden. Thus, it is possible that this sectioning issue may be at the root of the unexpected increase in internal surface area with increasing depth.

Fifth, the edges of the flats shaved on the specimens preferentially etch before the rest of the surface, see Figures 1(b) and 1(c).

And, sixth, some air bubbles can be observed, which have been trapped in the ice, see Figures 1(b) and 1(c).

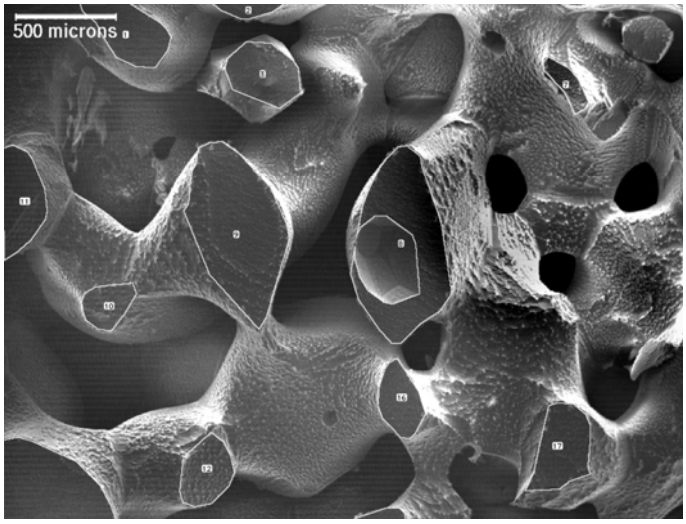

Figure 2. Secondary electron image of firn sample from 13.019 m. The boundaries of the pore areas were traced with the drawing tool, and the perimeter and enclosed area measured with the pixel-counting measurement utility of Image SXM (Barrett 2005).

Figure 3 shows a higher magnification image of two grains in firn. In this case, ridges (indicated) appear to have formed on either side of the grain boundary groove. Because the ridges were well below the surface of the ice, EDS analysis was not possible. Adams et al. (2001) observed a grain boundary ridge on snow crystals that were sintering together, a feature that they suggested was indicative of direct evidence for grain boundary diffusion as a sintering mechanism in ice. However, Barnes (2003) later pointed out that the ridge *may* have been a grain boundary impurity filament of the kind observed previously in ice (Baker and Cullen 2003a; 2003b; Baker et al. 2003; Baker et al. 2006; Barnes et al. 2002a; 2002b; Cullen and Baker 2000; 2001; 2002a; 2002b; Cullen et al. 2002; Iliescu et al. 2002; Iliescu and Baker 2004; Obbard et al. 2003a; 2003b).

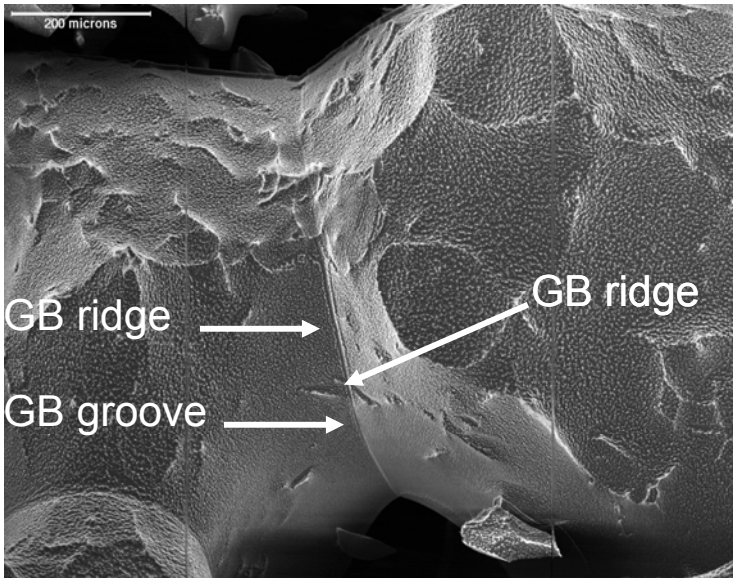

Figure 3. Higher-magnification secondary electron images of firn samples showing ridging on either side of a grain boundary groove (arrowed). The vertical lines are scan faults.

Figure 4 shows x-ray spectra taken from white spots formed during the sublimation of the surface of firn specimens. The oxygen peak is from the ice, while the carbon peak arises from the breakdown of diffusion pump oil under the electron beam in the SEM. In the shallow samples (9.71 m and 13.019 m), for example Figure 4(a), only small, barely-detectable quantities of impurities were found in the white spots. In this case, S and Cl were found. Spectra from white spots on deeper firn specimens showed more pronounced peaks. The example spectra shown in Figure 4(b) contain Cl, K, Na, S, Si and possibly Ca. Such impurities have often been noted in white spots in ice specimens from Greenland and Antarctica (Cullen and Baker 2001; 2002b Baker and Cullen 2003a; Barnes et al. 2002a; 2002b; Obbard et al. 2003a; 2003b; Baker et al. 2006). It is evident that impurities are spread throughout the firn. We did not find any impurities segregated to the grain boundaries as has been found in ice from Antarctica and Greenland (Cullen and Baker 2000; 2001; 2002b; Cullen et al. 2002; Barnes et al. 2002a; 2002b; Baker et al. 2003; Baker and Cullen 2003a; 2003b; Obbard et al. 2003a; 2003b; Baker et al. 2006).

Finally, Figure 5 shows an EBSP from firn from 3 m. The reds lines indicate the centers of the indexed Kikuchi bands. The pattern, while not as good quality as patterns previously presented for ice (Cullen and Baker 2002a; Iliescu et al. 2004; 2005; Obbard et al. 2006) is of sufficient quality that it is indexable. Various poles are indicated on the pattern. Each EBSP contain the complete three-dimensional orientation information of the crystal from whence it came and together the patterns enable the misorientations between grains to be determined.

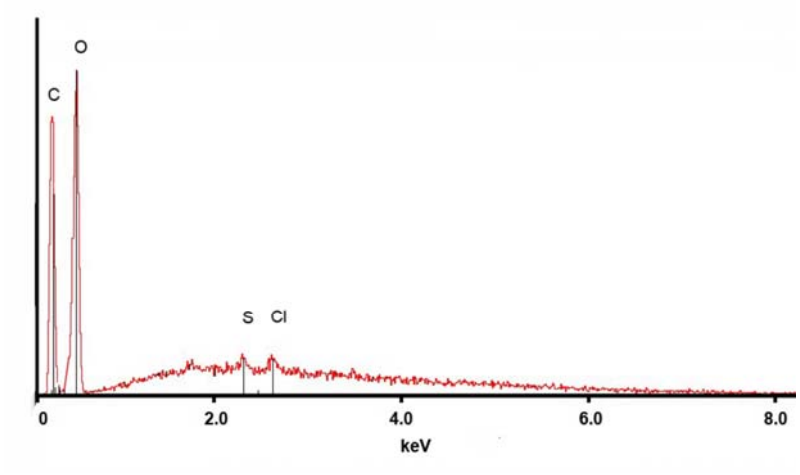

A

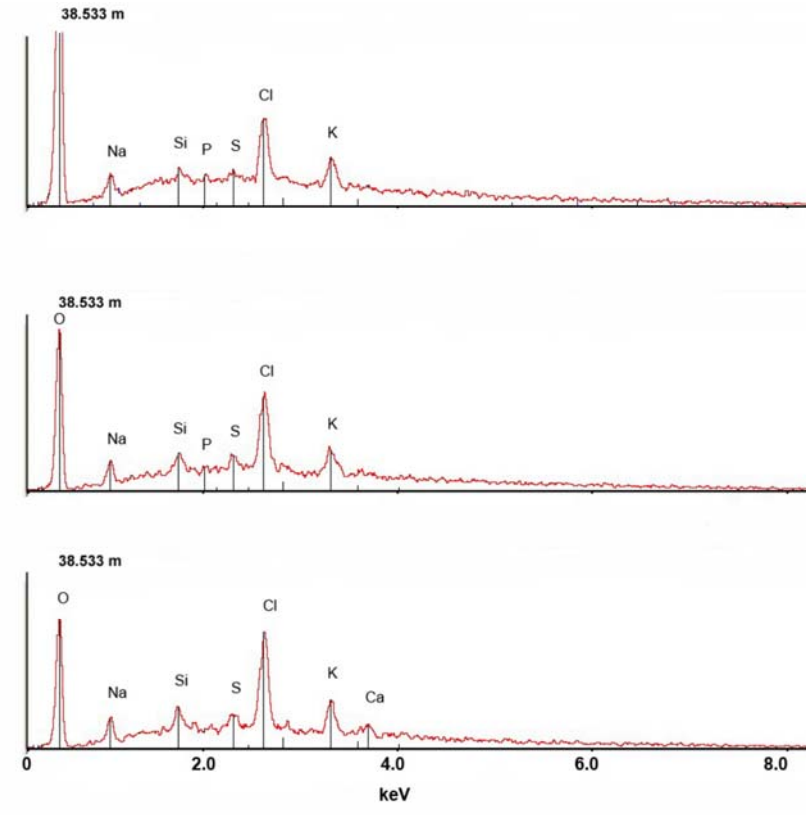

B

Figure 4. X-ray spectra taken from white spots, such as that indicated in Figure 1(c), on the surface of firn samples from depths of: (a) 9.71 m; and (b) 38.533 m. The full scale counts are 1130 for (a) and 230 from the three spectra in (b).

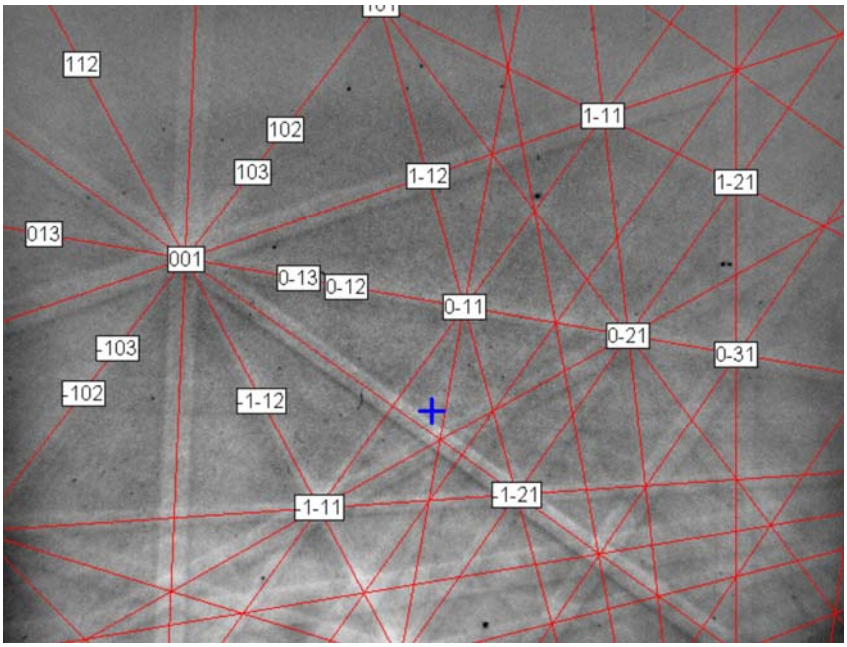

Figure 5. Indexed electron backscatter diffraction pattern from firn from a depth of 3 m.

CONCLUSION

In conclusion, we have shown that it is possible and useful, using various advanced electron-optical techniques and x-ray spectroscopy measurements in a SEM, to examine firn at high resolution. By observing grain boundary grooves, one can determine where snow crystals were joined; their orientations can be determined from EBSPs, allowing the misorientations between grains to be calculated; the porosity, approximate grain size and internal pore surface area can be measured; and the microchemistry of impurities can be determined by EDS.

ACKNOWLEDMENTS

The cores were collected during the 2005 US International Trans Antarctic Scientific Expedition and samples provided from NSF Grant 9980434. Support by the U.S. National Science Foundation Office of Polar Programs Grant 0440523 and U.S. Army Research Office under contract DAAD 19-03-1-0110 are gratefully acknowledged. The views and conclusions contained herein are those of the authors and should not be interpreted as necessarily representing official policies, either expressed or implied, of the National Institute of Standards and Technologies, or the U.S. Government.

REFERENCES

Adams EE, Miller DA, Brown RL. 2001. Grain boundary ridge on sintered bonds between ice crystals. *Journal of Applied Physics* **90**: 5782–5785.

Albert M, Shultz EF. 2002. Snow and firn properties and air–snow transport processes at Summit, Greenland. *Atmospheric Environment* **36**: 2789–2797.

Baker I, Cullen D. 2003a. The Structure and Chemistry of 94m GISP2 ice. *Annals of Glaciology* **35**: 224–230.

Baker I, Cullen D. 2003b. SEM/EDS observations of impurities in polar ice: artifacts or not? *Journal of Glaciology* **49**(16): 184–190.

Baker I, Cullen D, Iliescu D. 2003. The microstructural location of impurities in ice. Canadian *Journal of Physics* **81**: 1–9.
Baker I, Iliescu D, Obbard R, Chang H, Bostick B, Daghlian CP. 2006. Microstructural Characterization of Ice Cores. *Annals of Glaciology*, in press.
Barnes PRF, Mulvaney R, Robinson K, Wolff EW. 2002a. Observations of polar ice from the Holocene and the glacial period using the scanning electron microscope. *Annals of Glaciology* **35**: 559–566.
Barnes PRF, Mulvaney R, Wolff EW, Robinson K. 2002b. A technique for the examination of polar ice using the scanning electron microscope. *Journal of Microscopy* **205**: 118–124.
Barnes PRJ. 2003. Comment on "Grain boundary ridge on sintered bonds between ice crystals" [J. Appl. Phys. 90, 5782 (2001)]. *Journal of Applied Physics* **93**: 783–785.
Barnes PRJ, Wolff EW, Mallard DC, Meider HM. 2003. SEM Studies of the Morphology and Chemistry of Polar Ice. *Microscopy Research and Technique* **62**: 62–69.
Barrett S. 2005. Image SXM, Surface Science Research Centre, University of Liverpool, Liverpool, UK.
Cullen D, Baker I. 2000. The Chemistry of Grain Boundaries in Greenland Ice. *Journal of Glaciology* **46**: 703–706.
Cullen D, Baker I. 2001. Observation of Impurities in Ice. *Microscopy Research and Technique* **55**: 198–207.
Cullen D, Baker I. 2002a. Sulfate Crystallites in Vostok Accretion Ice. *Materials Characterization* **48**: 263–270.
Cullen D, Baker I. 2002b. Scanning Electron Microscopy of Vostok Acrretion Ice. In *Proceedings of Microscopy and Microanalysis*; 1546-7CD.
Cullen D, Iliescu D, Baker I. 2002. SEM/EDS Studies of Impurities in Natural Ice. In *Proceedings of Microscopy and Microanalysis*; 1398-9CD.
Fukazawa H, Sugiyama K, Mae S, Narita H, Hondoh T. 1998. Acid ions at triple junction of Antarctic ice observed by Raman scattering. *Geophysical Research Letters*, **25**: 2845.
Iliescu D, Baker I. 2002. Imaging of Uncoated Snow Crystals Using a Low-Vacuum Scanning Electron Microscope. *Journal of Glaciology* **48**(162): 479–480.
Iliescu D, Baker I, Cullen D. 2002. Preliminary Microstructural and Microchemical Observations of Pond and River Accretion Ice. *Cold Regions Science and Engineering* **35**: 81–99.
Iliescu D, Baker I. 2004. Characterization of the microstructure and mechanical properties in seasonal lake and river ice. In *Proc. 24th Army Science Conference*, Orlando, FL; OS-26.
Iliescu D, Baker I, Chang H. 2004. Determining the Orientations of Ice Crystals using Electron Backscatter Patterns. *Microscopy Research and Technique* **63**: 183–187.
Iliescu D, Baker I, Daghlian CP. 2005. Orientation Mapping in Polycrystalline Ice Using Electron Backscatter Patterns. In *Proceedings of Microscopy & Microanalysis*, Honolulu, HI; 1500–1501.
Mulvaney R, Wolff EW, Oates K. 1988. Sulphuric acid at grain boundaries in Antarctic ice. *Nature* **331**: 247.
Obbard R, Iliescu D, Cullen D, Chang J, Baker I. 2003a. SEM/EDS Comparison of Polar and Seasonal Temperate Ice. *Microscopy Research and Technique* **62**: 49–61.
Obbard R, Iliescu D, Baker I, Cullen D. 2003b. A Technique for the Scanning Electron Microscopy and Microanalysis of Uncoated Ice Crystals. In *Electron Microscopy: Its Role in Materials Science, The Mike Meshii Symposium*, TMS, Warrendale, PA; 133–140.
Obbard R, Baker I, Sieg K. 2006. Using Electron Backscatter Diffraction Patterns To Examine Recystallization in Polar Ice Sheets. Submitted to *Journal of Glaciology*.
Rasband W. S. 1997–2006. NIH ImageJ, http://rsb.info.nih.gov/ij/.
Rick U, Albert, M. 2004. Microstructure of West Antarctic Firn and its Effect on Air Permeability. ERDC/CREEL Report TR-04-16.
Underwood EE. 1970. Quantitative Stereology, Addision-Wesley Publishing Co., Reading, Mass, U.S.A., p24.
Wolff EW, Mulvaney R, Oates K. 1998. The location of impurities in Antarctic ice. *Annals of Glaciology*, **11**: 194.